Accurate Equilibrium Structures for Piperidine and Cyclohexane

7 AUTHORS, INCLUDING:

Patricia Écija
Universidad del País Vasco / Euskal Herriko U…
31 PUBLICATIONS   **198** CITATIONS

SEE PROFILE

Emilio José Cocinero
Universidad del País Vasco / Euskal Herriko U…
111 PUBLICATIONS   **1,182** CITATIONS

SEE PROFILE

Alberto Lesarri
Universidad de Valladolid
170 PUBLICATIONS   **2,373** CITATIONS

SEE PROFILE

Heinz Dieter Rudolph
Universität Ulm
113 PUBLICATIONS   **1,257** CITATIONS

SEE PROFILE

Accurate Equilibrium Structures for Piperidine and Cyclohexane

Jean Demaison,*,[†] Norman C. Craig,*,[‡] Peter Groner,[§] Patricia Écija,[∥] Emilio J. Cocinero,[∥] Alberto Lesarri,[⊥] and Heinz Dieter Rudolph[#]

[†]Laboratoire de Physique des Lasers, Atomes et Molécules, Université de Lille 1, 59655 Villeneuve d'Ascq Cedex, France

[‡]Department of Chemistry and Biochemistry, Oberlin College, Oberlin, Ohio 44074, United States

[§]Department of Chemistry, University of Missouri—Kansas City, Kansas City, Missouri 64110-2499, United States

[∥]Departamento de Química Física, Facultad de Ciencia y Tecnología, Universidad del País Vasco (UPV-EHU), Ap. 644, E-48080 Bilbao, Spain

[⊥]Departamento de Química Física y Química Inorgánica, Facultad de Ciencias, Universidad de Valladolid, E-47011 Valladolid, Spain

[#]Department of Chemistry, University of Ulm, D-89069 Ulm, Germany

S *Supporting Information*

ABSTRACT: Extended and improved microwave (MW) measurements are reported for the isotopologues of piperidine. New ground state (GS) rotational constants are fitted to MW transitions with quartic centrifugal distortion constants taken from ab initio calculations. Predicate values for the geometric parameters of piperidine and cyclohexane are found from a high level of ab initio theory including adjustments for basis set dependence and for correlation of the core electrons. Equilibrium rotational constants are obtained from GS rotational constants corrected for vibration—rotation interactions and electronic contributions. Equilibrium structures for piperidine and cyclohexane are fitted by the *mixed estimation* method. In this method, structural parameters are fitted concurrently to predicate parameters (with appropriate uncertainties) and moments of inertia (with uncertainties). The new structures are regarded as being accurate to 0.001 Å and 0.2°. Comparisons are made between bond parameters in equatorial piperidine and cyclohexane. Another interesting result of this study is that a structure determination is an effective way to check the accuracy of the ground state experimental rotational constants.
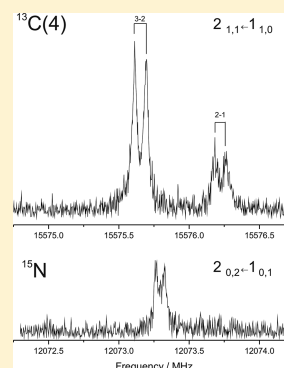
1. INTRODUCTION

The isoelectronic six-membered rings piperidine (azinane, $C_5H_{11}N$) and cyclohexane (C_6H_{12}) are chairlike in their lowest energy conformations.[1] In addition, the NH bond in piperidine is equatorial in the lower energy form. These two molecules are building blocks for many complex organic substances; so their structural study is well justified. The structures of piperidine and cyclohexane are shown schematically in Figures 1 and 2 along with their principal axes of rotation. Although the general features of the structures are well-known, accurate values of the

Figure 2. Structure of cyclohexane. The S_6 alternating axis of symmetry coincides with the principal axis c. Shown in gray is the plane perpendicular to the S_6 axis that passes through the center of symmetry. This plane helps define coordinates with full D_{3d} symmetry.
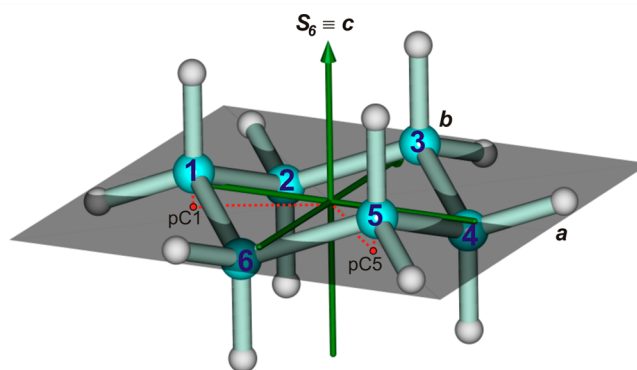
Figure 1. Structure of piperidine with its principal rotation axes. Atom 1 is nitrogen.

bond lengths and bond angles are yet to be found. In addition to determining equilibrium structures, a goal of this paper is to identify the subtle structural changes that occur when a nitrogen atom is introduced into a cyclohexane ring. Bond parameters with accuracies approaching 0.001 Å and 0.2° are essential for the comparison.

Finding equilibrium structures for piperidine and cyclohexane presents some problems. With only a plane of symmetry, piperidine has six different CH bonds, too many to interrogate by isotopic substitution. As in other nonplanar oblate tops, both molecules have a number of small Cartesian coordinates along the c axis of the principal axis system (PAS), thereby interfering with effective use of moments of inertia in a structure determination. Another consideration is that isotopic substitution in oblate tops may cause significant rotation of the PAS and consequent problems with structure fitting.[2] On the favorable side, a full set of ground state (GS) rotational constants is now available for all the heavy atom isotopologues of piperidine and the ND variant from microwave (MW) spectroscopy.[3−5] New MW observations reported in this paper improve this set of GS rotational constants. The structure of piperidine has been investigated by gas-phase electron diffraction (GED) by Gundersen and Rankin.[6]

For cyclohexane, which itself is nonpolar and thus MW silent, unsymmetrical isotopic substitutions gave five species with tiny dipole moments for a remarkable MW determination of the GS rotational constants of five species.[7] GS rotational constants ($A_0 = B_0$ only) were determined for the normal and perdeuterated species of cyclohexane with Raman spectroscopy, albeit with reduced accuracy compared with the MW results.[8] The rotational constants from these investigations were used by Kisiel and co-workers to determine ground state (r_0) and average (r') structures for cyclohexane.[9] A recent determination of the B_0 rotational constant for cyclohexane by Raman coherence spectroscopy by Brügger et al. led to an equilibrium structure without making use of the MW data.[10] GED studies by Bastiansen et al. and Schäfer et al. gave nonequilibrium structures for cyclohexane.[11,12] These GED studies and that for piperidine, although very useful when they were published, are now recognized as not very accurate or complete.

When the number of observed rotational transitions for a species is large and varied, it is generally easy to determine accurate GS rotational constants with proper fitting of centrifugal distortion constants. Furthermore, statistical tests may be used to check that the assignments are correct and that the least-squares fit gives reliable results. In contrast, when the number of observed transitions is small or not sufficiently varied, as is the usual situation for isotopic species, fits of rotational constants are no longer reliable. Centrifugal distortion constants have to be supplied, typically by transfer from the normal species or by quantum chemical (QC) calculations. It is now possible to make rather accurate estimates of centrifugal distortion constants for specific isotopologues from ab initio force fields. Then the method of mixed regression can be applied when fitting transitions to get GS rotational constants free from centrifugal distortion constant effects. The problem of confirming assignments of MW transitions is trickier. An auxiliary goal of this paper is to show that the process of determining a semiexperimental (SE) structure provides a solution to this assessment problem.[13,14] Such an assessment for piperidine led to remeasuring some MW lines and refitting the spectra. In addition, the MW lines for the ^{15}N species were measured for the first time.

An essential approach for the structure determinations reported in the present paper uses what is known as the *mixed estimation* method.[15,16] First, in this method, equilibrium structures are estimated with high-level QC calculations. These provisional bond parameters accompanied by reasonable estimates of uncertainties are then fitted concurrently with equilibrium rotational constants (with appropriate uncertainties) to determine the optimal structural parameters. The equilibrium rotational constants are derived from GS rotational constants and their vibration−rotation corrections computed with QC methods.[17,18]

2. EXPERIMENTAL SECTION

The rotational spectrum of piperidine was examined with a Balle−Flygare-type[19−21] Fourier transform microwave (FT-MW) spectrometer in Bilbao, operating in the frequency range 4−18 GHz.[22] Piperidine, which is liquid at room temperature, was vaporized by flowing a current of pure neon at backing pressures of ∼4 bar. The gas mixture expands quasi-adiabatically inside an evacuated Fabry−Perot resonator, forming a $T \approx 1−2$ K, pulsed supersonic jet. Short (microsecond) synchronous pulses of MW radiation coherently excite the molecular ensemble, resulting in a macroscopic polarization. The transient free induction decay (FID) accompanying relaxation is later digitized in the time domain and Fourier transformed to give the frequency domain spectrum, which contains the rotational resonances. The accuracy of the frequency measurements is better than 3 kHz. Transitions closer than approximately 10 kHz are resolvable. Because of the coaxial arrangement of the molecular jet and the resonator axis, the molecular transitions are split by a Doppler effect. Exceptional transitions may be seen in Figure 3. The rest frequencies reported here correspond to the average frequency of the Doppler doublet. Recording of the weak signals from the ^{13}C and ^{15}N isotopologues in natural abundance required integration times of up to 30 000 cycles.

3. COMPUTATIONAL DETAILS

The geometry optimizations of this study were performed at the MP2 (second-order Møller−Plesset perturbation theory)[23] and the CCSD(T) [coupled cluster theory, including single and double excitations (CCSD[24] augmented with a perturbational estimate of the effects of connected triple excitations)[25] levels of electronic structure theory. Different Gaussian basis sets have been utilized, including the correlation-consistent polarized triple- and quadruple-ζ basis sets, cc-pVTZ and cc-pVQZ,[26] abbreviated throughout this paper as VTZ and VQZ, respectively. Optimizations were also performed with the correlation-consistent polarized weighted core−valence triple-ζ, cc-pwCVTZ, and quadruple-ζ, cc-pwCVQZ,[27] basis sets, denoted here as wCVTZ and wCVQZ, respectively. With the wCVTZ and wCVQZ basis sets all of the electrons were correlated (AE), whereas with the VTZ and VQZ basis sets the frozen core approximation was normally used.

In order to determine the cubic force fields,[28] the MP2/VTZ level of theory was used. The Kohn−Sham density functional theory (DFT)[29] using Becke's three-parameter hybrid exchange functional[30] and the Lee−Yang−Parr correlation functional,[31] together denoted as B3LYP, was also employed. An ultrafine grid was selected for integrations. The cubic force fields were always determined for the tightly optimized equilibrium structures. All computations utilized the Gaussian 09 (G09) program suite.[32] Alpha/2 sums for calculating equilibrium rotational constants
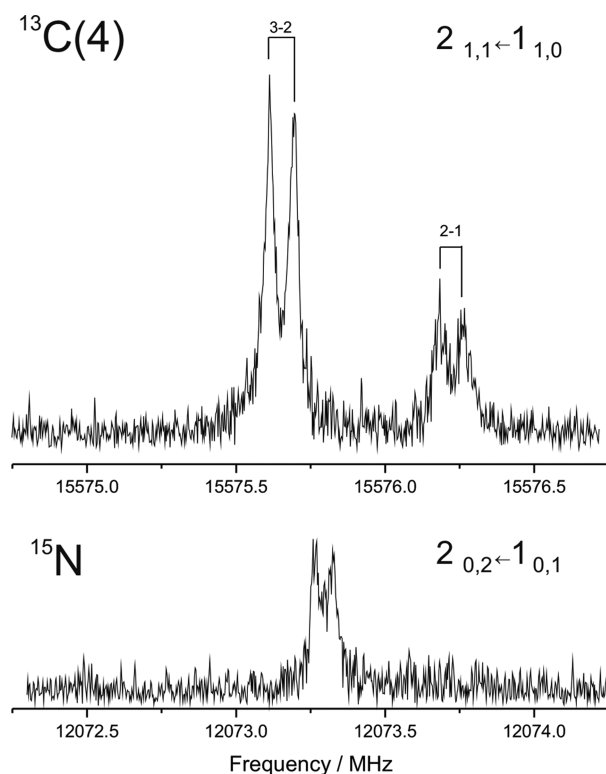
Figure 3. MW rotational transitions for two isotopic species of piperidine. These features are the results of tens of thousands of pulses. ^{14}N quadrupole coupling splits the line for the ^{13}C(4) species; corresponding F values are shown on the Doppler doublets.

there was a problem with the C_0 rotational constants of the 3-^{13}C and 4-^{13}C isotopic species; see section 6. For all these reasons, we made additional MW measurements and reanalyzed all the spectra. The analysis was made in three steps. First, the hyperfine structure was analyzed by direct diagonalization using Pickett's CALPGM suite of programs.[34] Then the deperturbed rotational frequencies corrected for the quadrupole effect were calculated. Because the number of measured transitions is small, it is not possible to determine most of the quartic centrifugal distortion constants. For this reason, we used the method of predicate observations, in which theoretical centrifugal distortion constants derived from a quadratic B3LYP/cc-pVTZ force field were used as supplementary data in a weighted least-squares fit to the transitions. The starting uncertainty of these predicate centrifugal distortion constants was 10% of their value. In all cases, an A-reduced Watson Hamiltonian in the representation I^r was used.[35] When only quartic centrifugal distortion constants are included in the fit, this choice of representation is suitable to give good values for A_0, B_0, and C_0 even for an oblate top.[36] In the last step, the experimental frequencies were directly fitted using as starting parameters the values determined in the previous two steps. The fitted GS rotational constants and the fitted centrifugal distortion constants are given in Table 1, and the experimental MW frequencies and residuals are in Table S1 of the Supporting Information.

5. AB INITIO STRUCTURES

The structure of piperidine was optimized at the frozen core (FC) CCSD(T)/VTZ level of theory. As convergence with respect to the basis set is not achieved with the VTZ set, the effects of further basis set improvement (VTZ → VQZ) were investigated at the MP2 level. This method is justified because the corrections are small. The core and core–valence correlation effects were estimated with the wCVQZ basis set at the MP2 level, which is accurate enough when there are only period 1 and 2 atoms.[37] Briefly, composite ab initio parameters were obtained using the following equation:

$$r_e^{BO} = r\{CCSD(T)/VTZ(FC) + MP2/[VQZ(FC) \\ - VTZ(FC) + wCVQZ(AE) - wCVQZ(FC)]\} \tag{1}$$

In this equation, BO means Born–Oppenheimer. The results are given in Table 2. It is worth noting that whereas the modest MP2/VTZ level of theory predicts the bond angles with an

from GS rotational constants were computed with program VIBROT.[17] The harmonic force constants were left unscaled.

4. ROTATIONAL SPECTRA OF PIPERIDINE

The GS rotational constants of the parent species of piperidine, of the N–D species, and of the three ^{13}C species were already known, but the centrifugal distortion constants of the parent species were inaccurate and were then fixed at the parent species values when fitting rotational constants for the isotopic species. This choice may have affected the accuracy of the rotational constants, whereas it is desirable to have rotational constants as accurate as possible to determine a reliable structure.[33] Furthermore, the rotational constants of the ^{15}N species were missing. Finally, during the first structural fits, it appeared that

Table 1. Ground State Rotational Parameters in an A-Reduction with an I^r Representation for the Different Isotopologues of Piperidine

		parent	^{15}N	2-^{13}C	3-^{13}C	4-^{13}C	D(N)^a
A_0	MHz	4527.22921(64)	4524.1826(23)	4484.27414(41)	4481.68431(64)	4525.44314(34)	4527.6200(11)
B_0	MHz	4437.23062(54)	4363.7247(19)	4398.18854(41)	4396.51495(35)	4353.28876(28)	4232.96710(65)
C_0	MHz	2542.98419(55)	2519.71492(75)	2517.93449(18)	2516.51898(21)	2515.85995(18)	2474.92407(77)
Δ_J	kHz	0.5792(43)	0.5705(30)	0.5595(15)	0.5566(15)	0.5687(13)	0.5185(43)
Δ_{JK}	kHz	−0.2978(21)	−0.3061(16)	−0.19408(53)	−0.18087(48)	−0.29939(69)	−0.2540(20)
Δ_K	kHz	0.7233(31)	0.7270(38)	0.5959(16)	0.5826(16)	0.7235(17)	0.7349(50)
δ_J	kHz	0.20788(71)	0.2005(10)	0.19507(54)	0.19383(52)	0.19961(46)	0.1799(13)
δ_K	kHz	0.3148(14)	0.3142(16)	0.34200(94)	0.34468(92)	0.31741(73)	0.3050(21)
$1.5\chi_{aa}$	MHz	3.1498(71)		3.3286(55)	3.3574(53)	3.150(13)	3.183(9)^b
$(\chi_{bb} - \chi_{cc})/4$	MHz	1.8989(25)		1.8711(15)	1.8658(14)	1.9025(28)	1.902(3)^b
no. trans.		92	4	32	23	18	7

^{a}Transitions were deperturbed for ^{14}N and ^{2}H quadrupole coupling. ^{b}From ref 4, ^{14}N quadrupole coupling constants.

Table 2. Structure of Piperidine[a]

	CCSD(T) VTZ	MP2 VTZ	MP2 VQZ	MP2/wCVQZ (FC)	(AE)	r_e^{BO}	r_e^{SE}
N–H	1.0137	1.0127	1.0110	1.0110	1.0096	1.0106	1.0116(3)
N–C2	1.4659	1.4598	1.4568	1.4564	1.4530	1.4595	1.4589(2)
C2–C3	1.5275	1.5215	1.5191	1.5187	1.5153	1.5217	1.5212(2)
C3–C4	1.5324	1.5261	1.5238	1.5233	1.5198	1.5266	1.5255(2)
C2–Hx	1.1048	1.1022	1.1012	1.1012	1.0996	1.1022	1.1020(5)
C2–Hq	1.0923	1.0897	1.0888	1.0887	1.0871	1.0898	1.0897(5)
C3–Hx	1.0945	1.0915	1.0906	1.0905	1.0889	1.0920	1.0918(5)
C3–Hq	1.0936	1.0909	1.0899	1.0898	1.0882	1.0910	1.0909(5)
C4–Hx	1.0970	1.0940	1.0930	1.0929	1.0913	1.0944	1.0943(5)
C4–Hq	1.0931	1.0904	1.0896	1.0895	1.0878	1.0906	1.0906(5)
HNC2	109.12	109.39	109.76	109.77	109.93	109.65	109.70(3)
C2NC6	110.94	110.94	111.21	111.22	111.32	111.31	111.34(2)
NC2C3	109.28	109.18	109.25	109.25	109.29	109.39	109.37(2)
C2C3C4	110.26	110.16	110.21	110.20	110.22	110.32	110.31(2)
C3C4C5	110.52	110.43	110.43	110.43	110.45	110.53	110.57(2)
NC2Hx	112.06	112.12	111.97	111.97	111.96	111.91	111.91(9)
NC2Hq	108.57	108.64	108.65	108.65	108.69	108.62	108.63(8)
C3C2Hx	108.75	108.71	108.69	108.69	108.68	108.71	108.67(12)
C3C2Hq	110.47	110.52	110.58	110.59	110.58	110.53	110.54(8)
C2C3Hx	108.52	108.48	108.52	108.52	108.52	108.56	108.56(12)
C2C3Hq	109.91	109.94	109.88	109.88	109.89	109.86	109.87(8)
C4C3Hx	109.65	109.69	109.69	109.69	109.69	109.65	109.64(9)
C4C3Hq	110.59	110.65	110.65	110.65	110.66	110.59	110.86(8)
C3C4Hx	109.00	109.01	109.02	109.03	109.03	109.02	109.02(4)
C3C4Hq	110.63	110.68	110.67	110.67	110.67	110.62	110.62(4)
HqC4Hx	106.97	106.94	106.93	106.93	106.89	106.92	106.91(11)
HNC2C3	176.19	175.54	175.03	175.02	174.80	175.47	175.38(7)
NC2C3C4	57.78	57.97	57.75	57.75	57.65	57.46	57.44(2)
HNC2Hx	−63.20	−63.93	−64.51	−64.52	−64.74	−64.00	−64.15(13)
HNC2Hq	−55.63	−54.95	−54.31	−54.29	−54.04	−54.75	−54.65(10)
C6NC2Hx	57.06	56.85	57.14	57.15	57.32	57.53	57.48(12)
C6NC2Hq	175.89	175.73	175.97	175.97	176.11	176.27	176.28(8)
NC2C3Hx	−62.33	−62.10	−62.37	−62.38	−62.48	−62.71	−62.72(8)
NC2C3Hq	−179.94	−179.84	−179.94	−179.94	−179.87	−179.97	−179.95(9)
C5C4C3Hq	−175.22	−175.55	−175.53	−175.54	−175.57	−175.23	−175.43(8)
C2C3C4Hx	66.31	65.95	65.97	65.96	65.97	66.34	66.33(8)
C2C3C4Hq	−176.34	−176.70	−176.69	−176.70	−176.73	−176.36	−176.39(9)

[a]x = axial; q = equatorial; distances in Å, angles in degrees.

Table 3. Structure of Cyclohexane[a]

| method: | CCSD(T) | MP2 | MP2 | MP2 | MP2 | CCSD(T) | MP2 | r_e^{BO}(I) [b] | r_e^{BO}(II) [c] | r_e^{SE} [d] | r_e^{SE} [e] |
basis set:	VTZ(FC)	VTZ(FC)	VQZ(FC)	wCVQZ(AE)	wCVQZ(FC)	wCVTZ(AE)	wCVTZ(AE)			CCSD(T)	
C–C	1.5326	1.5263	1.5240	1.5200	1.5235	1.5284	1.5217	1.5267	1.5267	1.526	1.5258(6)
C–Hx	1.0971	1.0941	1.0931	1.0914	1.0931	1.0953	1.0922	1.0945	1.0945	1.094	1.0957(4)
C–Hq	1.0937	1.0910	1.0901	1.0884	1.0900	1.0919	1.0891	1.0911	1.0912	1.0903	1.09137(7)
CCC	111.07	110.97	110.98	110.99	110.98	111.09	110.99	111.09	111.09	111.04	111.114(9)
CCHx	109.05	109.06	109.05	109.06	109.05	109.06	109.06	109.05	109.05	109.07	108.99(2)
CCHq	110.33	110.39	110.40	110.40	110.40	110.33	110.40	110.34	110.34	110.42	110.33(7)
HCH	106.91	106.87	106.86	106.82	106.85	106.86	106.82	106.86	106.86	106.73	106.98(13)
CCCC	55.87	56.14	56.11	56.08	56.11	55.80	56.08	55.80	55.80	55.98	55.73(3)

[a]Distances in Å; angles in degrees. [b]r_e^{BO}(I) = r{CCSD(T)/VTZ(FC) + MP2/[VQZ(FC) − VTZ(FC) + wCVQZ(AE) − wCVQZ(FC)]}. [c]r_e^{BO}(II) = r[CCSD(T)/wCVTZ(AE) + MP2/wCVQZ(AE) − MP2/wCVTZ(AE)]. [d]Ref 10. Mixed SE and ab initio method. [e]This work.

accuracy generally better than 0.3°, the error for the dihedral angles can be as large as 0.7°.

The structure of cyclohexane was calculated in the same way. It was also computed at the CCSD(T)/wCVTZ(AE) level of theory, the effect of basis set enlargement (wCVTZ → wCVQZ) being estimated with the MP2 method. The results are given in Table 3, where I and II represent the first and second methods, respectively. Both methods give almost identical results. Brügger

et al. published a CCSD(T)/ANO1 structure,[10] but this basis set is still too small to obtain a result close to the equilibrium value. In addition, the same authors calculated a semiexperimental structure based on the extrapolation of the computed rotational constants. Their structure is in very good agreement with ours and is also given in Table 3.

6. SEMIEXPERIMENTAL STRUCTURE OF PIPERIDINE

The semiexperimental equilibrium rotational constants, B_e, for each direction in the PAS were calculated from the experimental ground state rotational constants, B_0, using the following equation:

$$B_e = B_0 + \Delta B_{vib} + \Delta B_{el} \tag{2}$$

where ΔB_{vib} is the rovibrational correction calculated from the cubic force field[17] and ΔB_{el} is the electronic correction, which may be obtained from the rotational g tensor.[38] As the experimental values of the g-constants are not known, they were calculated at the B3LYP/6-311+G(3df,2pd) level of theory with G09. Their values for the normal species ($g_{aa} = -0.0115$; $g_{bb} = -0.0074$; and $g_{cc} = -0.0126$) are small and do not significantly affect the structure.

Twenty-four rotational constants were available, but this set is not sufficient for the structure of piperidine, which is defined by 25 independent parameters. In addition, no rotational constants for the C–D isotopologues were available. For this reason, the method of mixed estimation was used. The predicates are the best ab initio parameters determined in the previous section (data column 6 of Table 2) with a conservative uncertainty of 0.002 Å for the bond lengths, 0.3° for the bond angles, and 0.5° for the dihedral angles. These uncertainties come from a statistical analysis of the differences between structural parameters of CCSD(T)/VQZ quality and their experimental equilibrium values.[39,40] These numbers are confirmed by many studies; see for instance ref 41.

A first fit was performed with the parameters defining bond lengths and angles of the hydrogen atoms fixed at the their best ab initio values. This allowed us to estimate the accuracy of the semiexperimental rotational constants. In the least-squares fits, the following uncertainties (in MHz) were applied for the weighting: 0.1, 0.07, and 0.03 for A, B, and C, respectively. Note that these uncertainties are less than 0.2% of the rovibrational corrections; i.e., they are more than 1 order of magnitude smaller than the uncertainty generally associated with these rovibrational contributions.[42]

In the next fit, all parameters were fitted and the ab initio values of the various parameters defining the C–H bonds were used as predicates. The resulting fit was ill-conditioned because there were many small Cartesian coordinates and the number of data was not large compared to the number of fitted parameters. Hence, ab initio predicate values were used for all the fitted parameters, thereby considerably improving the conditioning of the fit. It was checked that the uncertainty assigned to the predicates was compatible with their residuals and that the residuals of the semiexperimental moments of inertia were not significantly increased. To sum up, at each step, a sophisticated analysis of the residuals[16] permitted checking of the appropriateness of the weights and the compatibility of the rotational constants and the predicate observations.

For the first fits the semiexperimental rotational constants were calculated using the published ground state rotational constants. The result was not satisfactory with very large residuals for the C rotational constants of isotopologues 3-^{13}C and 4-^{13}C.

Inspection of the P_b equilibrium planar moment of inertia $(1/2)(I_a + I_c - I_b)$, which should be invariant upon isotopic substitution for a species with an ac symmetry plane, confirmed that the rotational constants of the 4-^{13}C species were wrong. P_b for this species should be close to the 97.152 uÅ^2 value of the parent, ^{15}N and N–D species, as found with vib–rot corrections from the B3LYP/VTZ force field, whereas the observation-based value was 97.174 uÅ^2 for the 4-^{13}C species. See Tables S3 and S4 for P_b values for species with atoms substituted in the plane of symmetry. Errors in assignments of one transition for each the 3-^{13}C and 4-^{13}C species were found. The 3_{13}–2_{12} transition for the former was interchanged with the 3_{03}–2_{02} transition of the latter.[5] This finding prompted us to remeasure the MW spectra and refit the lines to GS rotational constants; see section 4. The new equilibrium rotational constants solve the problem and permit obtaining a good fit for the structure. The discovery of errors in the MW assignments in the course of structure fitting illustrates the power of this method.

The cubic force field was calculated at the MP2/VTZ and B3LYP/VTZ levels of theory. The optimized structures used for these calculations are given in Table S2 of the Supporting Information, and the semiexperimental rotational constants computed with the $\alpha/2$ sums and the electronic corrections are given in Tables S3 and S4 of the Supporting Information. The two force fields give compatible results; see Table S5 of the Supporting Information, which also gives the definitions of the fitted parameters. The fitted parameters and their variance–covariance matrix are used to determine the Cartesian coordinates of the atoms (given in Table S6 of the Supporting Information) as well as their variance–covariance matrix. These were, in turn, employed to calculate the internal coordinates and their standard deviations, as given in Table 2. Both transformations are nonlinear, and it may happen that an unfavorable propagation of errors affects the accuracy of some derived parameters. In particular, it may be the case for the bond angle $\angle$(C4C3Hq) and the torsional angle τ(C5C4C3Hq) whose SE values are noticeably different from the r_e^{BO} values. In this particular case, it appears that the r_e^{BO} values are already converged at the CCSD(T)/VTZ level of theory; see Table 2. Hence, they are likely to be more accurate than the SE values. Obviously, it would be possible to reduce this discrepancy by reducing the weight of the rotational constants, but it would give the misleading impression that the structure is extremely accurate.

Inspection of the residuals of the fits (Tables S3 and S4) and of the standard deviations of the fitted parameters (Table S5) indicates that the MP2/VTZ force field is slightly better. One likely explanation for this better behavior is that the MP2/VTZ structure is significantly closer to the equilibrium one than the B3LYP/VTZ structure. For instance, for the bond lengths the maximum deviation from the r_e structure is 0.002 Å (NH bond length) for the MP2/VTZ structure, whereas it is 0.006 Å (C2–C3 bond length) with the B3LYP/VTZ structure. For the bond angles the maximum deviations for the two models are 0.37° and 1.14° [$\angle$(C2NC6) angle in both cases], respectively. For the dihedral angles the maximum deviations for the two models are 0.68° [τ(HxC6NC2) angle] and 2.41° [τ(HxC3C2Hx) angle], respectively. See Table S2 of the Supporting Information. For this reason, only the semiexperimental equilibrium structure derived from the MP2/VTZ force field is given in the last column of Table 2. The values in the last column of Table 2 are the accepted structure with the exception of values for $\angle$(C4C3Hq)

and $\tau(C5C4C3Hq)$, for which the values in the r_e^{BO} column are preferred.

7. SEMIEXPERIMENTAL STRUCTURE OF CYCLOHEXANE

The structure of cyclohexane, which has high D_{3d} symmetry, is defined symmetrically by six parameters: four distances and two angles, which are related to the center of symmetry and a plane containing the center of symmetry and perpendicular to the S_6 symmetry axis. These coordinates are defined in association with Table S7 in the Supporting Information. See also Figure 2. These coordinates define, in turn, three bond lengths, which are C−C, C−H(ax), and C−H(eq), and three bond angles, which are C−C−H(ax), C−C−H(eq), and C−C−C(dihedral). The parent molecule is an oblate symmetric top.

The semiexperimental structure of cyclohexane has been determined by Brügger et al. by an interpolation method guided by the one observable GS rotational constant of the parent species to obtain the three independent bond lengths.[10] For each of the three kinds of bond lengths, predicted equilibrium rotational constants determined at two levels of CCSD(T)/ANO(X) theory were plotted linearly versus the bond length, and the corresponding predictions of GS rotational constants were plotted parallel. The one observed GS constant was used to select the predicted GS constant and the corresponding (r_e) bond length on each the three graphs. The three independent bond angles were then estimated from the ab initio calculations that gave the best estimates of the bond lengths. With only one experimental value, this method is heavily dependent on theory. This method appears to succeed because of the high D_{3d} symmetry of cyclohexane, which depends on only six parameters, and a weak dependence of bond angles on models. Up to now, the method has been tested on very few molecules and, furthermore, the agreement is not always convincing.[33]

Here we determine the semiexperimental structure of cyclohexane using the mixed estimation method. Doing so is easy in the present case because the rotational constants of the parent species[10] as well as a sufficient number of isotopic species[7,8] have been accurately determined. They were not refit. The structure of cyclohexane has been determined in the same way as that of piperidine; see the previous section.

As the experimental values of the g-constants are not known, they were calculated at the B3LYP/6-311+G(3df,2pd) level of theory with G09. Their values ($g_{aa} = -0.0044$; $g_{cc} = -0.0134$) are small and do not significantly affect the structure. The cubic force field has been calculated at two different levels of theory: MP2/VTZ (Table S8) and B3LYP/VTZ (Table S9). Tables S8 and S9 give the equilibrium rotational constants of the normal species and six deuterium isotopologues, including one with ^{13}C substitution. The optimized structures used for these calculations of cubic force constants are given in Table S10 of the Supporting Information, and the semiexperimental rotational constants are given in Tables S8 and S9 of the Supporting Information. Both force fields give compatible results. See Table S7 of the Supporting Information, which also gives the definitions of the fitted parameters. However, inspection of the residuals of the fits (Tables S8 and S9) and of the standard deviations of the fitted parameters (Table S7 and Figure 2) indicates that the MP2/VTZ force field is better as for piperidine. The preferred semi-experimental equilibrium structure for cyclohexane is in the last column of Table 3. The corresponding Cartesian coordinates are given in Table S11 of the Supporting Information.

8. DISCUSSION

It is interesting to note that in the particular case of these two molecules, the CH, CC, and CN bond lengths are accurately calculated at the MP2/VTZ level of theory, as is not the case for the B3LYP/VTZ method. For the CH bond, there is a large amount of documentation confirming that the MP2/VTZ CH bond lengths are generally accurate because of an auspicious compensation of errors.[41,43] The case of the CC and CN bonds is more interesting. The good result for these bonds is likely because they are single bonds.[44] This bond character is confirmed by the calculation of the bond ellipticity ε using the atoms in molecules (AIM) theory.[45,46] ε provides a measure of the extent to which the charge is preferentially accumulated at a given angle in a plane perpendicular to the bond path and, for this reason, is a measure of the π-character of the bond. ε is indeed found to be small, as is seen in Table S12 of the Supporting Information. The situation with MP2/VTZ theory is less pleasing for the bond angles and still worse for the dihedral angles. One might think that the addition of diffuse functions to the basis set should improve the result. However, an attempt to use the much larger aug-cc-VTZ basis set instead of the VTZ one does little to improve the situation. In comparison, the use of the 6-311++G(3df,2pd) basis set, which is not much larger than the VTZ one, permits calculating the bond angles with a better accuracy, the maximum deviation being 0.20° instead of 0.37° for VTZ. However, there is no improvement for the dihedral angles. Inspection of Table 2 indicates that the MP2 level of theory is not sufficient for an accurate prediction of the dihedral angles.

The accurate equilibrium structures for piperidine and cyclohexane permit close comparison of their bond parameters. The C−N bond length in piperidine is about 0.07 Å shorter than the C−C bond lengths in piperidine and in cyclohexane. The shorter C−N bond length reflects the shrinkage of the sp³ orbital of the nitrogen atom due to its greater electronegativity in comparison with the carbon atom. A substantial shortening of the N−H bond compared to the C−H bond occurs for the same reason.

In both piperidine and cyclohexane, the C−Hx bond length is longer than the C−Hq bond length in each case, as seen in Tables 2 and 3. The difference is ≥0.0037 Å except for the C3−H bonds in piperidine, where the difference is only 0.0009 Å. We will comment below on this small difference and the large difference of 0.0123 Å between C2−Hx and C2−Hq in piperidine.

The structure around atom C4 in piperidine, which is maximally distant from the nitrogen atom, is close to the structure of cyclohexane. In contrast, the methylene group at the C2 carbon atom in piperidene is quite asymmetric, CHx being longer by 0.0123 Å than CHq. This large difference is confirmed by the calculation, using the AIM theory, of the bond critical point density, ρ_b, which is a measure of the amount of electron density shared between the two bonded atoms; see Table S12 of the Supporting Information, where ρ_b for the C2−Hx bond is smaller than for all the other C−H bonds. The Hx···Hq distance is also significantly longer at the C2 carbon atom: 1.770 Å to be compared with 1.756 Å at the C4 carbon atom. The C3Hx bond is shorter by 0.0025 Å than the C4Hx bond, an outcome that might reflect some across-space interaction with the unshared pair of electrons on the nitrogen atom.

The lengthening of the C2Hx and C5Hx bonds is a consequence of the well-known effect of an unshared electron pair trans to the CH bond.[47] This effect, called the anomeric effect in sugars, causes a weakening and lengthening of a CH

F

dx.doi.org/10.1021/jp505765t | J. Phys. Chem. A XXXX, XXX, XXX−XXX

bond due to electron donation to the antibonding σ orbital of this bond. A concomitant effect is the shortening of the bond between the pair-donor atom and the carbon atom of the CH bond. To explore these effects on bond lengths in piperidine, the optimized structures of the axial and equatorial N—D conformers were computed with the MP2/cc-pVTZ model. The comparative results for the bond lengths of the two conformers are in Table S13. The C2Hx bond length in axial piperidine was 1.0939 Å compared with 1.1022 Å in equatorial piperidine. The C2Hq bond length was 1.0901 Å compared with 1.0897 Å, and the CN bond length was 1.4616 Å compared to 1.4598 Å. These results are in accord with the anomeric effect. The longer N—Hx bond length calculated for axial piperidine compared to the N—Hq bond length in equatorial piperidine is consistent with differences found for axial and equatorial C—H bonds.

Some structural parameters in piperidine may be compared with those in 1-methyl-4-piperidone.[44] 1-Methyl-4-piperidone has an equatorial methyl group attached to the nitrogen atom and a carbonyl group at C4. Despite these significant changes, reasonable agreement exists between the N—C2, C2—C3, C2—Hx, and C2—Hq bond lengths of the two molecules (numbering from piperidine). For piperidine and 1-methyl-4-piperidone the bond lengths (Å) are respectively the following: N—C2, 1.459 and 1.456; C2—C3, 1.521 and 1.527; C2—Hx, 1.102 and 1.103; C2—Hq, 1.090 and 1.0905. The largest difference of 0.006 Å reflects the influence of the carbonyl bond on the C2—C3 bond length The effect of the unshared pair of electrons of the nitrogen atom on increasing the C2—Hx bond length is very close in the two molecules.

9. CONCLUSIONS

Accurate equilibrium structures for the chair forms of piperidine (equatorial NH) and cyclohexane have been determined. The bond parameters, regarded as good to 0.001 Å and 0.2°, are given in Tables 2 and 3. These quantities have been determined from a mixed estimation fit to predicate (ab initio) bond parameters and equilibrium moments of inertia, each data set accompanied by appropriate uncertainties. The accurate bond parameters reveal the subtle effects of nitrogen substitution in the cyclohexane ring. The most important effect is the significant lengthening of the C—Hx axial bond vicinal to the point of the nitrogen atom substituent. The difference in bond length reflects the trans interaction of the unshared electron pair on nitrogen with the antibonding orbital of the C—Hx bond. The C—N bond length is shorter than the C—C bond lengths and the N—H bond length is shorter than C—H bond lengths owing to the greater electronegativity of the nitrogen atom.

ASSOCIATED CONTENT

ⓢ Supporting Information

Thirteen tables listing MW transitions, rovibrational corrections for piperidine and cyclohexane, ab initio calculations for piperidine and for cyclohexane with different models, definitions of parameters used in fitting bond parameters, atoms in molecules analysis for piperidine, a comparison of ab initio predictions for piperidine with axial and equatorial NH bonds, and equilibrium Cartesian coordinates for piperidine and cyclohexane. This material is available free of charge via the Internet at http://pubs.acs.org.

AUTHOR INFORMATION

Corresponding Authors

*J.D.: e-mail, Jean.Demaison@gmail.com.

*N.C.C.: e-mail, Norm.Craig@oberlin.edu.

Notes

The authors declare no competing financial interest.

ACKNOWLEDGMENTS

REFERENCES

(1) Riddell, F. G. *The Conformational Analysis of Heterocyclic Compounds*; Academic Press: London, 1980.

(2) Demaison, J.; Császár, A. G.; Margulès, L.; Rudolph, H. D. Equilibrium Structures of Heterocyclic Molecules with Large Principal Axis Rotations upon Isotopic Substitution. *J. Phys. Chem. A* **2011**, *115*, 14078−14091.

(3) Parkin, J. E.; Buckley, P. J.; Costain, C. C. The Microwave Spectrum of Piperidine: Equatorial and Axial Ground States. *J. Mol. Spectrosc.* **1981**, *89*, 465−483.

(4) Ehrlichmann, H.; Grabow, J.-U.; Dreizler, H.; Heineking, N.; Andolfatto, M. Nitrogen and Deuterium Hyperfine Structure in the Rotational Spectrum of Piperidine. *Z. Naturforsch., A* **1989**, *44*, 841−847.

(5) Spoerel, U.; Stahl, W. Equatorial Piperidine and the Piperidine-Water Complex. Rotational Spectra and Molecular Structures. *Chem. Phys.* **1998**, *239*, 97−108.

(6) Gundersen, G.; Rankin, D. W. H. The Gas-Phase Molecular Structure of Piperidine Studied by Electron Diffraction. *Acta Chem. Scand., Ser. A* **1983**, *37*, 865−874.

(7) Dommen, J.; Brupbacher, Th.; Grassi, G.; Bauder, A. Microwave Spectra of Isotopic Species and Substitution Structure of Cyclohexane. *J. Am. Chem. Soc.* **1990**, *112*, 953−957.

(8) Peters, R. A.; Walker, W. J.; Weber, A. High Resolution Raman Spectroscopy of Gases with Laser Sources. VII: The Rotational Spectrum of Cyclohexane-C_6H_{12} and C_6D_{12}. *J. Raman Spectrosc.* **1973**, *1*, 159−176.

(9) Białkowska-Jaworska, E.; Jaworski, M.; Kisiel, Z. The Structure of Cyclohexane, F-, Cl-, Br- and I-Cyclohexane. *J. Mol. Spectrosc.* **1995**, *350*, 247−254.

(10) Brügger, G.; Frey, H.-M.; Steinegger, P.; Kowalewski, P.; Leutwyler, S. Femtosecond Rotational Raman Coherence Spectroscopy of Cyclohexane in a Pulsed Supersonic Jet. *J. Phys. Chem. A* **2011**, *115*, 12380−12389.

(11) Bastiansen, O.; Fernholt, L.; Seip, H. H.; Kambara, H.; Kuchitsu, K. Structure of Cyclohexane Determined by Two Independent Gas Electron-Diffraction Investigations. *J. Mol. Struct.* **1973**, *18*, 163−168.

(12) Ewbank, J. D.; Kirsch, G.; Schäfer, L. Electron-Diffraction Study of Hydrogen Isotope Effects in Cyclohexane. *J. Mol. Struct.* **1976**, *31*, 39−45.

(13) Pawłowski, F.; Jørgensen, P.; Olsen, J.; Hegelund, F.; Helgaker, T.; Gauss, J.; Bak, K. L.; Stanton, J. F. Molecular Equilibrium Structures from Experimental Rotational Constants and Calculated Vibration−Rotation Interaction Constants. *J. Chem. Phys.* **2002**, *116*, 6482−6496.

(14) Vázquez, J.; Stanton, J. F. Semiexperimental Equilibrium Structures: Computational Aspects. In *Equilibrium Molecular Structures*; Demaison, J., Boggs, J. E., Császár, A. G., Eds.; CRC Press: Boca Raton, FL, 2011; pp 53−87.

(15) Belsley, D. A. . *Conditioning Diagnostics*; Wiley: New York, 1991.

(16) Demaison, J. The Method of Least Squares. In *Equilibrium Molecular Structures*; Demaison, J., Boggs, J. E., Császár, A. G., Eds.; CRC Press: Boca Raton, FL, 2011; pp 29−52.

(17) Groner, P.; Warren, R. D. Approximate r_e Structures from Experimental Rotational Constants and ab Initio Force Fields. *J. Mol. Struct.* **2001**, *509*, 323−335.

(18) Clabo, D. A.; Allen, W. D.; Remington, R. B.; Yamaguchi, Y.; Schaefer, H. F., III. A Systematic Study of Molecular Vibrational Anharmonicity and Vibration-Rotation by Self-Consistent-Field Higher-Derivative Methods. Asymmetric Top Molecules. *Chem. Phys.* **1988**, *123*, 187−239.

(19) Balle, T. J.; Flygare, W. H. Fabry−Pérot Cavity Pulsed Fourier Transform Microwave Spectrometer with a Pulsed Nozzle Particle Source. *Rev. Sci. Instrum.* **1981**, *52*, 33.

(20) Grabow, J.-U. Fourier Transform Microwave Spectroscopy Measurement and Instrumentation. In *Handbook of High-Resolution Spectroscopy*; Quack, M., Merkt, F., Eds.; Wiley: Chichester, U.K., 2011; Vol. 2, Chapter 1.

(21) Grabow, J.-U.; Caminati, W. Microwave Spectroscopy: Experimental Techniques. In *Frontiers of Molecular Spectroscopy*; Laane, J., Ed.; Elsevier: Amsterdam, The Netherlands, 2009; Chapter 14.

(22) Cocinero, E. J.; Lesarri, A.; Écija, P.; Grabow, J.-U.; Fernández, J. A.; Castaño, F. Conformational Equilibria in Vanillin and Ethylvanillin. *Phys. Chem. Chem. Phys.* **2010**, *12*, 12486−12493.

(23) Møller, C.; Plesset, M. S. Note on an Approximation Treatment for Many-Electron Systems. *Phys. Rev.* **1934**, *46*, 618−622.

(24) Purvis, G. D., III; Bartlett, R. J. A Full Coupled-Cluster Singles and Doubles Model: The Inclusion of Disconnected Triples. *J. Chem. Phys.* **1982**, *76*, 1910−1918.

(25) Raghavachari, K.; Trucks, G. W.; Pople, J. A.; Head-Gordon, M. A Fifth-Order Perturbation Comparison of Electron Correlation Theories. *Chem. Phys. Lett.* **1989**, *157*, 479−483.

(26) Dunning, T. H., Jr. Gaussian Basis Sets for Use in Correlated Molecular Calculations. I. The Atoms Boron through Neon and Hydrogen. *J. Chem. Phys.* **1989**, *90*, 1007−1023.

(27) Woon, D. E.; Dunning, T. H., Jr. Gaussian Basis Sets for Use in Correlated Molecular Calculations. V. Core-Valence Basis Sets for Boron through Neon. *J. Chem. Phys.* **1995**, *103*, 4572−4585.

(28) Császár, A. G. Anharmonic Molecular Force Fields. *Wiley Interdiscip. Rev.: Comput. Mol. Sci.* **2012**, *2*, 273−289.

(29) Kohn, W.; Sham, L. J. Self-Consistent Equations Including Exchange and Correlation Effects. *Phys. Rev. A* **1965**, *140*, 1133−1138.

(30) Becke, A. D. Density-Functional Thermochemistry. III. The Role of Exact Exchange. *J. Chem. Phys.* **1993**, *98*, 5648−5652.

(31) Lee, C. T.; Yang, W. T.; Parr, R. G. Development of the Colle-Salvetti Correlation-Energy Formula into a Functional of the Electron Density. *Phys. Rev. B* **1988**, *37*, 785−789.

(32) Frisch, M. J.; Trucks, G. W.; Schlegel, H. B.; Scuseria, G. E.; Robb, M. A.; Cheeseman, J. R.; Scalmani, G.; Barone, V.; Mennucci, B.; Petersson, G. A.; et al. *Gaussian 09*, revision B.01; Gaussian Inc.: Pittsburgh, PA, 2010.

(33) Rudolph, H. D.; Demaison, J.; Császár, A. G. Accurate Determination of the Deformation of the Benzene Ring upon Substitution: Equilibrium Structures of Benzonitrile and Phenylacetylene. *J. Phys. Chem. A* **2013**, *117*, 12969−12982.

(34) Pickett, H. M. The Fitting and Prediction of Vibration-Rotation Spectra with Spin Interactions. *J. Mol. Spectrosc.* **1991**, *148*, 371−377.

(35) Watson, J. K. G. In *Vibrational Spectra and Structure*; Durig, J. R., Ed.; Elsevier: Amsterdam, 1977; Vol. *6*, pp 1−89.

(36) Margulès, L.; Motiyenko, R. A.; Alekseev, E. A.; Demaison, J. Choice of the Reduction and the Representation in Centrifugal Distortion Analysis: A Case Study of Dimethylsulfoxide. *J. Mol. Spectrosc.* **2010**, *260*, 23−29.

(37) Margulès, L.; Demaison, J.; Rudolph, H. D. Ab Initio and Experimental Structures of CH_3NC. *J. Mol. Struct.* **2001**, *599*, 23−30.

(38) Gordy, W.; Cook, R. L. *Microwave Molecular Spectra*; Wiley: New York, 1984; Chapter 11.

(39) Helgaker, T.; Gauss, J.; Jörgensen, P.; Olsen, J. The Prediction of Molecular Equilibrium Structures by the Standard Electronic Wave Functions. *J. Chem. Phys.* **1997**, *106*, 6430−6440.

(40) Lee, T. J.; Scuseria, G. E. Achieving Chemical Accuracy with Coupled-Cluster Theory. In *Quantum Mechanical Electronic Structure Calculations with Chemical Accuracy*; Langhoff, S. R., Ed.; Kluwer: Dortrecht, The Netherlands, 1995; Vol. *13*, pp 47−108.

(41) Demaison, J. Experimental, Semi-Experimental and ab Initio Equilibrium Structures. *Mol. Phys.* **2007**, *105*, 3109−3138.

(42) Vogt, N.; Vogt, J.; Demaison, J. Accuracy of the Rotational Constants. *J. Mol. Struct.* **2011**, *988*, 119−127.

(43) Demaison, J.; Craig, N. C. Semiexperimental Equilibrium Structure for *cis,trans*-1,4-Difluorobutadiene by the Mixed Estimation Method. *J. Phys. Chem. A* **2011**, *115*, 8049−8054.

(44) Demaison, J.; Craig, N. C.; Cocinero, E. J.; Grabow, J.-U.; Rudolph, H. D. Semiexperimental Equilibrium Structures for the Equatorial Conformers of *N*-Methylpiperidone and Tropinone by the Mixed Estimation Method. *J. Phys. Chem. A* **2012**, *116*, 8684−8692.

(45) Gillespie, R. J.; Popelier, P. L. A. *Chemical Bonding and Molecular Geometry*; Oxford University Press: Oxford, U.K., 2001.

(46) Bader, R. F. W. *Atoms in Molecules: A Quantum Theory*; Clarendon Press: Oxford, U.K., 1990.

(47) McKean, D. C. Individual CH Bond Strengths in Simple Organic Compounds: Effects of Conformation and Substitution. *Chem. Soc. Rev.* **1978**, *7*, 399−422.